

# 7A.2 THE EFFECTS OF HIGH HORIZONTAL RESOLUTION ON TROPICAL CYCLONES' POTENTIAL INTENSITY AND UPPER OCEAN HEAT CONTENT IN THE COMMUNITY EARTH SYSTEM MODEL

Jinjun Liu\* <sup>1</sup> and Robert Korty<sup>1</sup>

<sup>1</sup>Department of Atmospheric Sciences, Texas A&M University, College Station, TX

## 1. INTRODUCTION

With advancements in high-performance computing, there is a transition to high-resolution (HR) models due to their improved representation of climate mean states and tropical cyclones (TCs), as evidenced by early-stage research (e.g., Broccoli and Manabe 1990) and recent HR climate modeling efforts (e.g., Chang et al. 2020). Pioneering studies have demonstrated that HR can improve the model TCs within general circulation models (GCMs). For instance, Bower and Reed (2024) investigated the effects of climate change on TCs and their post-tropical cyclone (PTC) stages using three HighResMIP models' data, finding a consensus on fewer TC and PTC events in future warming scenarios but inconsistencies in regional changes and storm intensity evolution, while noting an increase in heavy rain rates and a corresponding rise in accumulated rainfall from these events.

However, most modern climate models continue to utilize relatively coarse resolutions, owing to the necessity of balancing improving the model resolution with meeting the requirements to run simulations over many years. For instance, the horizontal resolution of climate models in the recent World Climate Research Programme (WCRP) Coupled Model Intercomparison Project Phase 6 (CMIP6) typically ranges from nominal 1° to 2.5° horizontal resolution, albeit with some exceptions (Eyring et al. 2016; Han et al. 2021). It is generally considered that models have better skills in simulating large-scale environmental conditions as opposed to TCs themselves. E.g., Camargo et al. (2007) demonstrated that while there is a strong relationship between the model genesis index (based on large-scale environmental conditions) and observed TC variability, the correlation between the frequency of model-simulated TCs and the mean genesis index is relatively weak. This suggests that even though low-resolution models might not precisely simulate individual TCs, they are capable of accurately capturing large-scale environmental variables. Consequently, it is believed that low-resolution models can still be utilized to make future TC projections effectively.

This perspective faces challenges due to persistent errors in the simulation of tropical sea surface temperatures (SSTs) within climate models. Specifically, Camargo and Wing (2015) reviewed advancements in simulating TCs within climate models and argued that a significant chal-

lenge lies in producing reliable projections of future SST changes and their patterns, which are crucial for forecasting changes in TC frequency accurately in decadal time scale. Sobel et al. (2023) examined the CMIP6 data and argue that both high and low-resolution coupled models have inaccurately captured the transient dynamics of tropical Pacific SSTs. Whereas historical observations indicate a trend towards increasingly frequent La Niña events, these models have erroneously predicted a shift towards more frequent El Niño events. This discrepancy undermines their capability to accurately forecast regional changes in the climatology of TCs. Coats and Karnauskas (2018) highlight the importance of correctly modeling the equatorial undercurrent (EUC) to accurately simulate SSTs. Specifically, they emphasize the need to account for the cooling effects in the eastern equatorial Pacific, which result from the EUC's response to the equatorial zonal wind stress.

Most recently, researches indicate that HR simulations conducted using Community Earth System Model version 1.3 (CESM1.3) have enhanced the representation of large-scale ocean features (e.g., SSTs) in several ways. For instance, Xu et al. (2022) observed that the global mean SST in the CESM1.3 HR simulations is, on average, 1°C warmer compared to the lower resolution (LR) simulations, resulting in diminished SST biases. This improvement in SST is primarily attributed to a more accurate depiction of nonlocal vertical mixing and the management of shortwave heat flux in the HR simulations. Similarly, Li et al. (2022) demonstrated that HR simulations offer a more reliable projection of sea-level rise, particularly due to the improved simulation of the Gulf Stream along the eastern coast of the United States.

In addition to SSTs, the upper ocean also plays a critical role in interactions with TCs, serving as the primary interface for their development and intensification. The warmth of the upper ocean acts as a source of energy for TC formation, while the storm-induced mixing of water can bring colder water from the thermocline to the surface, leading to a reduction in sea surface temperature. Consequently, the vertical temperature profile of the upper ocean is a key factor in both the development and rapid intensification of TCs, as well as in the feedback mechanisms between TCs and the ocean itself (Korty et al. 2008; Balaguru et al. 2015; Potter et al. 2019). Therefore, accurate simulations of the upper ocean heat content and its response to climate change are critical for reliable future projections of TC activity.

\*Corresponding author address: Jinjun Liu, Department of Atmospheric Sciences, Texas A&M University, College Station, Texas 77843-3150; E-mail: jjliu@tamu.edu.

In this study, we aim to examine the effects of the horizontal resolution of climate models, with a particular focus on ocean model resolution, on SSTs and upper ocean heat content. We will also explore how SST in turn influences the potential intensity of TCs. This research will offer valuable insights into whether enhancing ocean resolution and improving the SST field can impact the projection of TC trends under future climate change scenarios.

## 2. DATA AND METHODS

This research primarily utilizes data from the CESM1.3 to investigate the influence of horizontal resolution on the TCs' potential intensity (PI) and upper ocean heat content. In addition, we incorporate data from six other models associated with the European PRIMAVERA project (Process-based climate sIMulation: AdVances in high-resolution modelling and European climate Risk Assessment) to corroborate the findings from CESM1.3. The PRIMAVERA models follow the protocols established by the High Resolution Model Intercomparison Project (HighResMIP) (Haarsma et al. 2016). These simulations feature at least two different resolution configurations to isolate the effects attributable to the model resolution while keeping other configuration aspects minimal changes. The specific resolutions employed in our study for each model are listed in Table 1.

Model name	Resolution names	Atmosphere horizontal resolutions	Ocean horizontal resolutions
CESM1.3	LR, HR	1°, 0.25°	1°, 0.1°
HadGEM3-GC3.1	LL, HH	2.5°, 0.5°	1°, 1/12°
ECMWF-IFS	LR, HR	0.5°, 0.25°	1°, 0.25°
CNRM-CM6-1	LR, HR	2.5°, 1°	1°, 0.25°
EC-Earth3P	LR, HR	1°, 0.5°	1°, 0.25°
CMCC-CM2-(V)HR4	HR4, VHR4	1°, 0.25°	0.25°, 0.25°
MPI-ESM1.2	HR, XR	1°, 0.5°	0.5°, 0.5°

TABLE 1. CESM and Six PRIMAVERA model horizontal resolutions

### 2.1. CESM1.3

The International Laboratory for High-Resolution Earth System Prediction (iHESP) project employs a dedicated version of CESM1.3 to perform a set of simulations (Chang et al. 2020). CESM1.3 integrates a fully coupled atmosphere-ocean-ice system, consisting of the Community Atmosphere Model version 5.2 (CAM5.2), the Paral-

lel Ocean Program version 2 (POP2), the Community Ice Code version 4 (CICE4), and the Community Land Model version 4 (CLM4). These simulations were carried out using both standard (low) resolution (hereafter referred to as LR) and high resolution (hereafter referred to as HR). The LR configuration features a 1° resolution in the atmospheric model and a nominal 1° resolution in both the ocean and sea-ice models. Conversely, the HR configuration boasts finer resolutions of 0.25° in the atmospheric model and 0.1° in the ocean and sea-ice models (Chang et al. 2020; Xu et al. 2022).

For this study, we selected the 250-year (1850-2100) historical and future transient simulation, hereinafter referred to as 1850-TNST, as our principal dataset. The choice is motivated, firstly, by the fact that the 1850-TNST branched off from the 1850 control simulation at year 250, thereby ensuring a prolonged spin-up time of 250 years that allows the ocean model to achieve a near-equilibrium state, thus minimizing model drift. Secondly, the extensive time span of the dataset, covering two and a half centuries, provides a uniquely lengthy timeframe to examine the effects of model resolution on tropical cyclones, an opportunity that is unparalleled in previous studies (Chang et al. 2020). The 1850-TNST simulation applies historical forcings from 1850 to 2005 and follows the Representative Concentration Pathway 8.5 (RCP8.5) projections from 2006 to 2100 (Chang et al. 2020). It should be noted that the future simulation forcing in the CESM1.3 is different from the PRIMAVERA models' future forcing - Shared Socioeconomic Pathways 585 (SSP585).

### 2.2. PRIMAVERA models

In this study, we incorporate data from six models within the PRIMAVERA project, namely HadGEM3-GC3.1 (Roberts et al. 2019), ECMWF-IFS (Roberts et al. 2018), CNRM-CM6-1 (Voltaire 2019), EC-Earth3P (Haarsma et al. 2020), CMCC-CM2-(V)HR4 (Cherchi et al. 2019), and MPI-ESM1.2 (Gutjahr et al. 2019). Some models feature more than two resolution options; in such cases, we select the lowest and highest resolutions for our comparison to accentuate the contrast between low-resolution (LR) and high-resolution (HR) simulations. For example, HadGEM3-GC3.1 provides a tiered resolution system (low, L; medium, M; high, H) for both its ocean and atmosphere components, yielding five possible combinations (i.e., LL, MM, HM, MH, HH) where the first letter represents the atmospheric model resolution and the second letter represents the ocean model resolution (Roberts et al. 2019). In this context, we use the LL configuration as our LR set and the HH configuration as our HR set. The ECMWF-IFS model offers three distinct resolution settings: ECMWF-IFS-HR, ECMWF-IFS-MR, and ECMWF-IFS-LR. Notably, the ECMWF-IFS-HR (ECMWF-IFS-LR) setup encompasses HR (LR) for both atmospheric and ocean modeling, while the MR option employs an LR atmospheric model coupled with an HR

ocean model (Roberts et al. 2018). For our purposes, we use data from the ECMWF-IFS-HR and ECMWF-IFS-LR only.

The PRIMAVERA model experiments follow the protocols outlined by the High Resolution Model Intercomparison Project (HighResMIP). This includes a series of experiments designed to facilitate the comparison of climate models at different resolutions:

1. spinup-1950: A brief simulation spanning 30-50 years, using averaged ocean temperature and salinity to force the models. This step establishes initial conditions for subsequent experiments, control-1950 and hist-1950.
2. control-1950: A simulation run with constant forcings representative of the 1950s, extended over a minimum duration of 100 years.
3. hist-1950: A historical experiment with forcings from 1950 until 2014, the conclusions of which are used to initialize the highres-future experiment.
4. highres-future: A projection using the SSP585 future scenario forcing, covering the period from 2015 to 2050 (Haarsma et al., 2016; Roberts et al., 2020).

Our study primarily focuses on the hist-1950 and highres-future experiments since they provide a continuous simulation spanning a full century.

### 2.3. Potential intensity

PI is the upper bound of tropical cyclone intensity for a given environmental condition (i.e., sea surface temperature, sea level pressure, atmosphere condition profile) (Emanuel 1986; Bister and Emanuel 1998). PI is statistically linked to the lifetime maximum of observed storms (Emanuel 2000). Therefore, it is widely used to assess the climatology of storms in various climate simulations (e.g. Korty et al. 2017; Lawton et al. 2021; Wu and Korty 2022). Recent studies show that large values of PI are becoming more frequent and have covered a larger area over the North Atlantic in the past 40 years (Wu and Korty 2022), which may pose more risks to the people living in coastal areas. As mentioned earlier, we calculate the monthly PI in the simulations using the script of an open-source Python library (Gilford 2021) and use the maximum wind speed ( $V_m$ ) of storms to represent PI. It is calculated using the following expression:

$$PI = \sqrt{\frac{C_K}{C_D} \frac{SST}{T_0} (CAPE^* - CAPE^b)} \quad (1)$$

where  $C_K$  and  $C_D$  are the exchange coefficients for enthalpy and drag, respectively,  $SST$  is sea surface temperature,  $T_0$  is the outflow temperature when convective air reaches saturation, CAPE is the convective available potential energy (CAPE). Superscript  $*$  is used for the CAPE of an air parcel lifted from saturation at the sea level pressure in reference to the local environmental sounding. Subscript  $b$  is used for the CAPE of an ambient boundary layer parcel.

### 2.4. Upper Ocean Heat Content Parameters

The thermal profile of the ocean is a critical factor in the development and rapid intensification of TCs, as the enthalpy flux from the ocean surface to the atmosphere is a direct source of energy for TCs. Conversely, TCs can cause the upper layers of the ocean to mix, leading to a reduction in water temperature. To explore the extent to which the interactions between TCs and upper ocean layers are captured in model simulations at different horizontal resolutions, this study examines several indicators related to the upper ocean's heat content and its impact on TCs. We compare these indicators across models with high resolution (HR) and low resolution (LR). The indicators include the ocean heat potential, the depth of the mixing layer, and the length of variable mixing.

Potter et al. (2019) defined the Tropical Cyclone Heat Potential (TCHP) using the following equation:

$$Q = c_p \sum_{Z_0}^{Z_{26}} \rho_i (T_i - 26) \Delta z_i, \quad (2)$$

where  $c_p$  represents the specific heat of seawater at constant pressure,  $T_i$  denotes the water temperature in degrees Celsius at the  $i$ -th level,  $\Delta z_i$  is the thickness of the water layer at the  $i$ -th level (assumed to be 50 cm), and  $\rho_i$  is the water density at the  $i$ -th level.  $Z_0$  and  $Z_{26}$  define the surface and the depth (in meters) respectively, where the 26 °C isotherm is found. The TCHP measures the available heat energy below the ocean's surface that can potentially fuel a tropical cyclone.

Balaguru et al. (2015) formulated an expression for the variable mixing length resulting from TC wind forcing as follows:

$$L = h + \left( \frac{2\rho_0 u_*^3 t}{\kappa g \alpha} \right)^{\frac{1}{3}}, \quad (3)$$

where  $h$  represents the initial mixed layer depth,  $\rho_0$  denotes the sea water density,  $u_*$  is the friction velocity,  $t$  signifies the mixing duration,  $\kappa$  is the von Kármán constant,  $g$  stands for the gravitational acceleration, and  $\alpha$  is the rate at which potential density increases with depth beneath the mixed layer. This relationship bears similarity to that derived by Korty et al. (2008), where the variable mixing length exhibits an approximate linear dependence on the wind force while showing a more weaker dependence on stratification. Furthermore, they calculated the vertically averaged temperature over the variable mixing length:

$$T_{dy} = \frac{1}{L} \int_0^L T(z) dz, \quad (4)$$

where  $T(z)$  represents the temperature at depth  $z$ . Balaguru et al. (2015) demonstrated that the computed Potential Intensity (PI) when replaced with  $T_{dy}$ -termed the Dynamic Potential Intensity (DPI)-provides a more accurate explanation for the variance in TC intensification than the original PI.

In this study, we aim to compare the variables  $Q$ ,  $h$ ,  $L$ , and  $T_{dy}$  between HR and LR simulations to investigate the specific mechanisms responsible for the disparities.

### 3. RESULTS

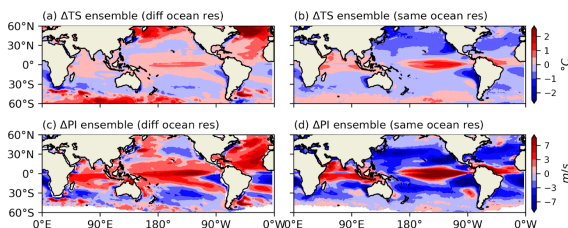


FIG. 1. The multi-model storm season historical long-term mean ensemble of  $\Delta TS$  (TS difference, defined as HR TS minus LR TS; a & b) and  $\Delta PI$  (similar to  $\Delta TS$ , but for PI; c & d) in the historical simulation (1950-2014) of the four PRIMAVERA models with different ocean model resolution (HadGEM3-GC3.1, ECMWF-IFS, CNRM-CM6-1, and EC-Earth3P; a & c), and two PRIMAVERA models with the exact ocean model resolution (CMCC-CM2-(V)HR4, and MPI-ESM1.2; b & d). Fields in all models are regridded to  $2.5^\circ \times 2.5^\circ$  to make ensembles.

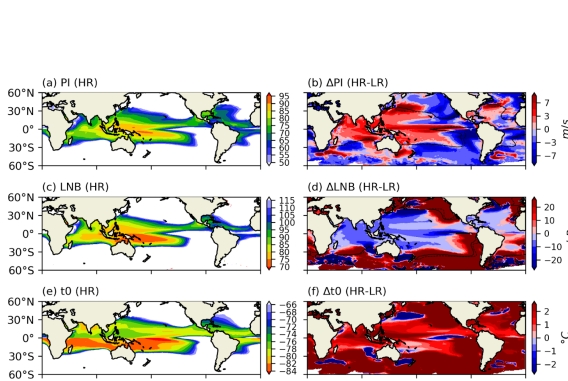


FIG. 2. Long-term means of (left) HR and (right) HR minus LR (HR-LR) for (a), (b) PI; (c), (d) LNB; (e), (f) outflow temperature ( $t_0$ ) in historical run (1950-2005) in storm season. Contours in panel b represent  $PI=50$  m/s, and in panel d, they represent  $LNB=500$  hPa. The solid lines correspond to HR, while the dashed lines correspond to LR.

### 4. CONCLUSION

1. SST differences in HR and LR simulations significantly influence the PI distribution in different ocean basins. These differences can be attributed to both ab-

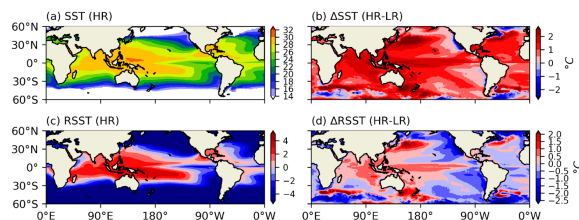


FIG. 3. Long-term means of (left) HR and (right) HR minus LR (HR-LR) for (a), (b) absolute SST; (c), (d) RSST in historical run (1950-2005) in storm season.

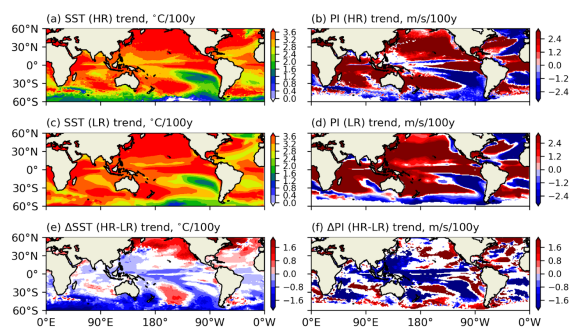


FIG. 4. The linear trends of (a) HR SST, (b) HR PI, (c) LR SST, (d) LR PI, (e) SST differences between HR and LR, and (f) PI differences between HR and LR in storm season during 2006-2100 in CESM 1850-TNST. “100y” stands for 100 years. Grids with color are significant at a 95% confidence level. A 1-D Gaussian filter (kernel size=11, sigma=2) is applied to the time series before linear regression.

solute SST and relative SST differences in HR and LR simulations. 2. Simulated PI differences between HR and LR increase in historical scenario but decrease in future scenario. 3. Heat potential, variable mixing length, and  $T_{dy}$  are larger in HR simulation than in LR, indicating TCs are easier to intensify in HR simulations.

*Acknowledgments.* Portions of this research were conducted with the advanced computing resources provided by Texas A&M High Performance Research Computing.

### REFERENCES

Baloguru, K., G. R. Foltz, L. R. Leung, E. D. Asaro, K. A. Emanuel, H. Liu, and S. E. Zedler, 2015: Dynamic potential intensity: An improved representation of the ocean’s impact on tropical cyclones.

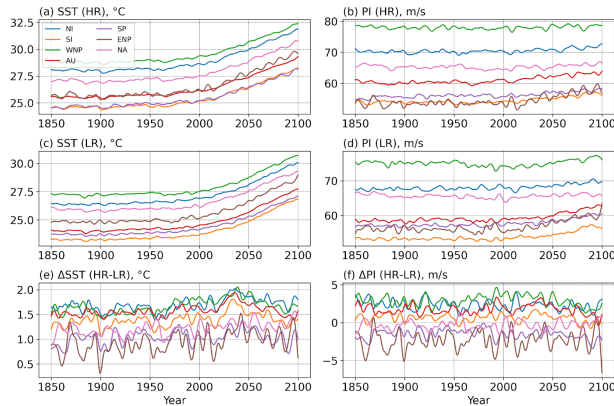


FIG. 5. CESM 1850-TNST simulation (1850-2100) annual mean time series in storm season (a) HR SST; (b) HR PI; (c) LR SST; (d) LR PI; (e)  $\Delta SST$  (HR-LR); and (f)  $\Delta PI$  (HR-LR) in different ocean basins. An 11-year 1-D Gaussian filter ( $\sigma=2$ ) is applied to the time series.

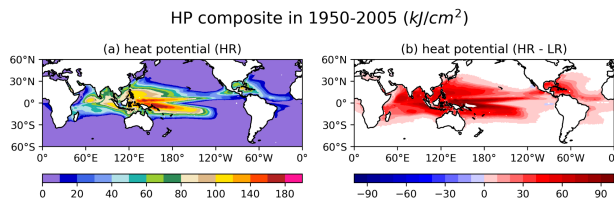


FIG. 6. Long-term means of (left) HR and (right) HR minus LR (HR-LR) for heat potential in historical run (1950-2005) in storm season.

*Geophysical Research Letters*, **42** (16), 6739–6746, doi:10.1002/2015gl064822.

Bister, M., and K. A. Emanuel, 1998: Dissipative heating and hurricane intensity. *Meteorology and Atmospheric Physics*, **65** (3–4), 233–240, doi:10.1007/bf01030791.

Bower, E., and K. A. Reed, 2024: Using high resolution climate models to explore future changes in post-tropical cyclone precipitation. *Environmental Research Letters*, **19** (2), 024042, doi:10.1088/1748-9326/ad2163.

Broccoli, A. J., and S. Manabe, 1990: Can existing climate models be used to study anthropogenic changes in tropical cyclone climate? *Geophysical Research Letters*, **17** (11), 1917–1920, doi:10.1029/g1017i011p01917.

Camargo, S. J., A. H. Sobel, A. G. Barnston, and K. A. Emanuel, 2007: Tropical cyclone genesis potential index in climate models. *Tellus A: Dynamic Meteorology and Oceanography*, **59** (4), 428, doi:10.1111/j.1600-0870.2007.00238.x.

Camargo, S. J., and A. A. Wing, 2015: Tropical cyclones in climate models. *WIREs Climate Change*, **7** (2), 211–

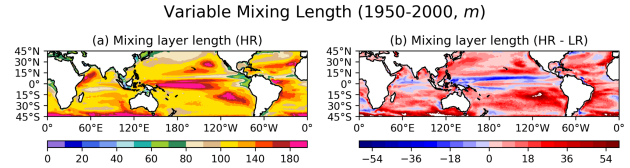


FIG. 7. Long-term means of (left) HR and (right) HR minus LR (HR-LR) for variable mixing length in historical run (1950-2000) in storm season.

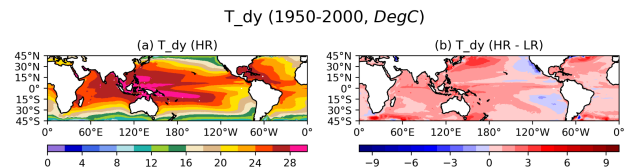


FIG. 8. Long-term means of (left) HR and (right) HR minus LR (HR-LR) for  $T_{dy}$  (vertically integrated temperature within variable mixing length) in historical run (1950-2000) in storm season.

237, doi:10.1002/wcc.373.

Chang, P., and Coauthors, 2020: An unprecedented set of high-resolution earth system simulations for understanding multiscale interactions in climate variability and change. *Journal of Advances in Modeling Earth Systems*, **12** (12), doi:10.1029/2020ms002298.

Cherchi, A., and Coauthors, 2019: Global mean climate and main patterns of variability in the cmcc-cm2 coupled model. *Journal of Advances in Modeling Earth Systems*, **11** (1), 185–209, doi:10.1029/2018ms001369.

Coats, S., and K. B. Karnauskas, 2018: A role for the equatorial undercurrent in the ocean dynamical thermostat. *Journal of Climate*, **31** (16), 6245–6261, doi:10.1175/jcli-d-17-0513.1.

Emanuel, K. A., 1986: An air-sea interaction theory for tropical cyclones. part i: Steady-state maintenance. *Journal of the Atmospheric Sciences*, **43** (6), 585–605, doi:10.1175/1520-0469(1986)043<0585:aasitf>2.0.co;2.

Eyring, V., S. Bony, G. A. Meehl, C. A. Senior, B. Stevens, R. J. Stouffer, and K. E. Taylor, 2016: Overview of the coupled model intercomparison project phase 6 (cmip6) experimental design and organization. *Geoscientific Model Development*, **9** (5), 1937–1958, doi:10.5194/gmd-9-1937-2016.

Gilford, D. M., 2021: pypi (v1.3): Tropical cyclone potential intensity calculations in python. *Geoscientific Model Development*, **14** (5), 2351–2369, doi:10.5194/gmd-14-2351-2021.

Gutjahr, O., D. Putrasahan, K. Lohmann, J. H. Jungclauss, J.-S. von Storch, N. Brüggemann, H. Haak, and

- A. Stössel, 2019: Max planck institute earth system model (mpi-esm1.2) for the high-resolution model inter-comparison project (highresmip). *Geoscientific Model Development*, **12** (7), 3241–3281, doi:10.5194/gmd-12-3241-2019.
- Haarsma, R., and Coauthors, 2020: Highresmip versions of ec-earth: Ec-earth3p and ec-earth3p-hr – description, model computational performance and basic validation. *Geoscientific Model Development*, **13** (8), 3507–3527, doi:10.5194/gmd-13-3507-2020.
- Haarsma, R. J., and Coauthors, 2016: High resolution model intercomparison project (highresmip v1.0) for cmip6. *Geoscientific Model Development*, **9** (11), 4185–4208, doi:10.5194/gmd-9-4185-2016.
- Han, Y., M.-Z. Zhang, Z. Xu, and W. Guo, 2021: Assessing the performance of 33 cmip6 models in simulating the large-scale environmental fields of tropical cyclones. *Climate Dynamics*, **58** (5–6), 1683–1698, doi:10.1007/s00382-021-05986-4.
- Korty, R. L., K. A. Emanuel, M. Huber, and R. A. Zamora, 2017: Tropical cyclones downscaled from simulations with very high carbon dioxide levels. *Journal of Climate*, **30** (2), 649–667, doi:10.1175/jcli-d-16-0256.1.
- Korty, R. L., K. A. Emanuel, and J. R. Scott, 2008: Tropical cyclone-induced upper-ocean mixing and climate: Application to equable climates. *Journal of Climate*, **21** (4), 638–654, doi:10.1175/2007jcli1659.1.
- Lawton, Q. A., R. L. Korty, and R. A. Zamora, 2021: Tropical cyclones downscaled from simulations of the last glacial maximum. *Journal of Climate*, **34** (2), 659–674, doi:10.1175/jcli-d-20-0409.1.
- Li, Y., Y. Tang, R. Toumi, and S. Wang, 2022: Revisiting the definition of rapid intensification of tropical cyclones by clustering the initial intensity and inner-core size. *Journal of Geophysical Research: Atmospheres*, **127** (20), doi:10.1029/2022jd036870.
- Potter, H., S. F. DiMarco, and A. H. Knap, 2019: Tropical cyclone heat potential and the rapid intensification of hurricane harvey in the texas bight. *Journal of Geophysical Research: Oceans*, **124** (4), 2440–2451, doi:10.1029/2018jc014776.
- Roberts, C. D., R. Senan, F. Molteni, S. Boussetta, M. Mayer, and S. P. E. Keeley, 2018: Climate model configurations of the ecmwf integrated forecasting system (ecmwf-ifs cycle 43r1) for highresmip. *Geoscientific Model Development*, **11** (9), 3681–3712, doi:10.5194/gmd-11-3681-2018.
- Roberts, M. J., and Coauthors, 2019: Description of the resolution hierarchy of the global coupled hadgem3-gc3.1 model as used in cmip6 highresmip experiments. *Geoscientific Model Development*, **12** (12), 4999–5028, doi:10.5194/gmd-12-4999-2019.
- Sobel, A. H., and Coauthors, 2023: Near-term tropical cyclone risk and coupled earth system model biases. *Proceedings of the National Academy of Sciences*, **120** (33), doi:10.1073/pnas.2209631120.
- Voltaire, A., 2019: Cnrm-cerfacs cnrm-cm6-1-hr model output prepared for cmip6 highresmip. Earth System Grid Federation, doi:10.22033/ESGF/CMIP6.1387.
- Wu, Y., and R. L. Korty, 2022: Changes in the length of the season with favorable environmental conditions for tropical cyclones in the north atlantic basin during the last 40 years. *Journal of Climate*, **35** (16), 5237–5256, doi:10.1175/jcli-d-21-0767.1.
- Xu, G., and Coauthors, 2022: Impacts of model horizontal resolution on mean sea surface temperature biases in the community earth system model. *Journal of Geophysical Research: Oceans*, **127** (12), doi:10.1029/2022jc019065.